A Three-Terminal ZnS-based CIGS Solar Cell

Shih-Chin Huang[1], Jyi-Tsong Lin[1], Steve Haga[2], Wen-Hao Chen [1] and Kung-Yu Ho [1]
[1]Department of Electrical Engineering/ [2]Department of Computer Science and Engineering
National Sun Yat-Sen University, 80424 Kaohsiung, Taiwan
Email: jtlin@ee.nsysu.edu.tw

Abstract

This paper presents new solar cell architecture, the double-sided copper indium gallium selenide (DS-CIGS) solar cell. The device introduces a third terminal between the two CIGS sides, comprised of a layer of conductive indium tin oxide (ITO). Being transparent, the ITO layer allows light to pass through and be absorbed by the CIGS cell on the other side. Designed for bifacial applications, simulation results indicate a 68.3% increase in conversion efficiency for equal front and back illumination, versus a comparable conventional bifacial CIGS architecture (η=29.68 % versus η=17.64 %).

1. Introduction

$CuIn_{1-x}Ga_xSe_2$ (CIGS) is one of the most promising light-absorbing materials for thin-film solar cells. By adjusting the proportion of indium to gallium, the direct band-gap energy can be adjusted anywhere between 1 eV ($CuInSe_2$) and 1.7 eV ($CuGaSe_2$).

Figure 1 presents the basic structure of a CIGS solar cell [1]. As shown, the buffer above the CIGS absorber is commonly made of cadmium sulfide. Due to cadmium's environmental concerns, however, Cd-free and low-Cd CIGS technologies have long term investment potential [1]-[3]. One alternative, Zinc oxysulfide ($ZnO_{1-x}S_x$) is already in production and has achieved comparable efficiency [4]-[6]. Also as shown, the aluminum contacts on the top surface must have their area minimized, so that they do not block much light from entering the cell.

Recently, interest in bifacial solar cells has increased, particularly for high ambient light conditions or high albedo environments. Bifacial versions of CIGS solar cells have been proposed [7]. Regarding the monofacial solar cell of Fig. 1, the reflective back contact prevents light from entering through the back surface. (It does have the advantage, however, of reflecting light from the front, thus giving the absorber region a second chance at capturing that light.) To allow light to enter from the back surface, a transparent conductor is need and the rear contacts must be distanced apart in the same way that the front surface's aluminum contact already were.

Fig. 2 presents one possible implementation of a bifacial CIGS+ solar cell [8]. The dimensions and doping levels given in this figure are those used in the simulations of this paper. The specific values were determined by optimization for our proposed device. As can be seen in the figure, indium-tin oxide, a transparent conductive oxide (TCO) allows light to enter the back surface.

2. Design and Simulation

Building on the concept of the bifacial CIGS solar cell, Fig. 3 presents our proposed double-sided CIGS (DS-CIGS) solar cell. The device is formed by placing a symmetrically inverted copy of the CIGS device on the bottom.

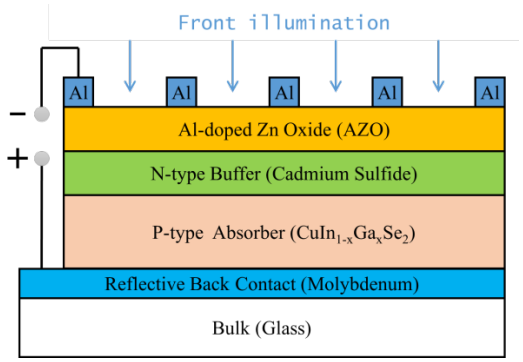

Figure 1. The general design of a traditional CIGS solar cell. The materials indicated are typically, but not universally, used. In particular, the CdS buffer can be replaced with zinc oxysulfide [1].

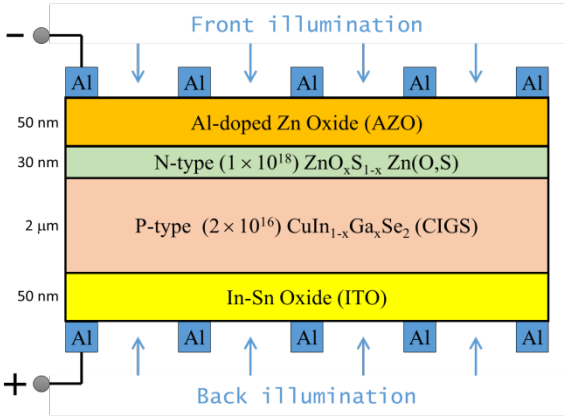

Figure 2. The Bifacial CIGS+ solar cell that we compare our results against. The doping concentrations and dimensions indicated are the same as for our device.

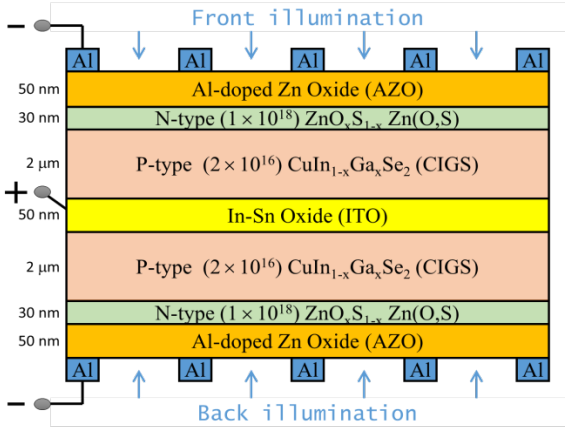

Figure 3. The Proposed Double-sided CIGS device. The DS CIGS is a three terminal device, as the central ITO layer forms the positive terminal. Light passing through the transparent ITO (from either top or bottom) has a second opportunity for absorption, within the CIGS absorber on the other side.

978-1-5386-4441-6/18/$31.00 ©2018 IEEE

The conductive ITO layer that lies in the middle of this new structure forms a third terminal. To reduce resistance in this ITO layer, it is made sufficiently thick (50nm) and a surround contact is used. With negative terminals now distributed on two sides, it can be anticipated that there will be a current mismatch, given that more light is likely to enter the front surface. If a somewhat closer match is desired, however, the doping levels and device thicknesses could be adjusted according to the anticipated albedo level.

In fact, all of the parameters in Fig. 3 can be adjusted. If, for example, the CIGS absorbers are too thick then recombination will reduce the obtained current. If, however, the absorbers are too thin, then an overly high amount of light will pass through without capture. The doping levels also affect these results. The device parameters shown were chosen based on device simulation optimizations.

All simulations were performed with the Silvaco ATLAS simulator. The full set of simulator parameters are provided in Table I. These parameters were obtained from real measurements for a monofacial CIGS cell [9] As shown, the solar cell was modeled as operating under a global standard solar spectrum (AM 1.5G) illumination with a total incident power density of 100 mW/cm^2 and a light intensity calculated for wavelengths from 300 nm to 1200 nm.

TABLE I.
The device parameters used for simulating our DS-CIGS solar cell. These parameters were obtained from measurement on a tradition CIGS solar cell [9]

Parameters	ZnS	CIGS
Energy gap (eV)	3.8	1.15
Doping density (cm^{-3})	1×10^{18} (donor)	2×10^{16} (acceptor)
Electron mobility (cm^2/Vs)	165	100
Hole mobility (cm^2/Vs)	5	25
Electron life time (s)	1	1×10^{-7}
Hole life time (s)	1	1×10^{-7}
Effective conduction band density (cm^{-3})	1	2.2×10^{18}
Effective valence band density (cm^{-3})	6.35×10^{19}	1.8×10^{19}
Permittivity (F/m)	8.3	13.6
Affinity (eV)	4.59	4.58

3. Results and Discussion

Table II compares the efficiency of the CIGS+ and DS-CIGS. When illuminated from the front only, the DG-CIGS solar cell achieves short circuit current, J_{sc}, that is 5.5 mA/cm^2 higher than the CIGS+. This is because the bottom cell of the DS-CIGS has a second absorber region that provides a second chance at capturing photons. The V_{oc} of the DS-CIGS is 0.013V lower, however, due to resistance loss. This resistance arises because the positive terminal of the DS-CIGS is made only of ITO, and lacks the aluminum strips of the CIGS+ device.

TABLE II.
Efficiencies of the CIGS + and DS-CIGS solar cells, under the illumination from the front or back sides.

Solar cell	V_{oc} (V)	J_{sc} (mA/cm^2)	FF (%)	η (%)
CIGS+ Front	0.603	29.60	80.80	14.44
CIGS+ Back	0.563	6.35	78.53	2.81
DS-CIGS Front	0.590	35.10	80.12	16.60
DS-CSIGS Back	0.582	25.54	81.44	12.11

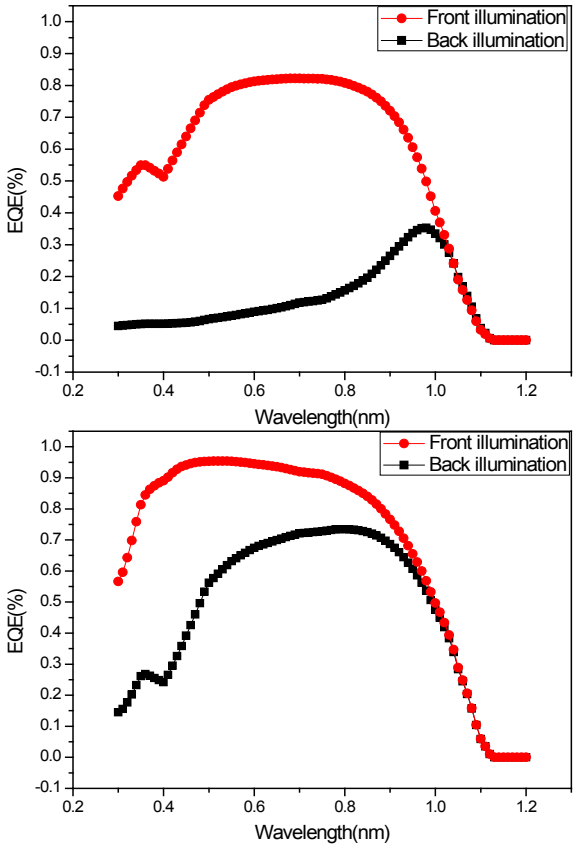

Figure 4. The EQE spectra for front illumination and back illumination. (a) The bifacial CIGS+ solar cell of Fig. 2. (b) The DS-CIGS solar cell of Fig.3.

Fig. 4 compares the External Quantum Efficiency (EQE) of the CIGS+ and DS-CIGS. Front and back illumination are considered separately, to observe each device's sensitivity to illumination from each surface; the true response of each device to a more-realistic combination of both illumination sources can be obtained by simple superposition of the illuminations considered separately.

As Fig 4(a) shows, the CIGS+ device performs poorly for back illumination. This is attributable in part to a large absorption loss at the back side of ClGS absorber layer which occurs because the energy bandgap prevents some photons from penetrating the Zn (O, S) layer. Another possible reason is that the photo-generated carriers cannot reach the junction near the CIGS absorber region. The DS-CIGS improves on the device and displays good characteristic performance under back illumination.

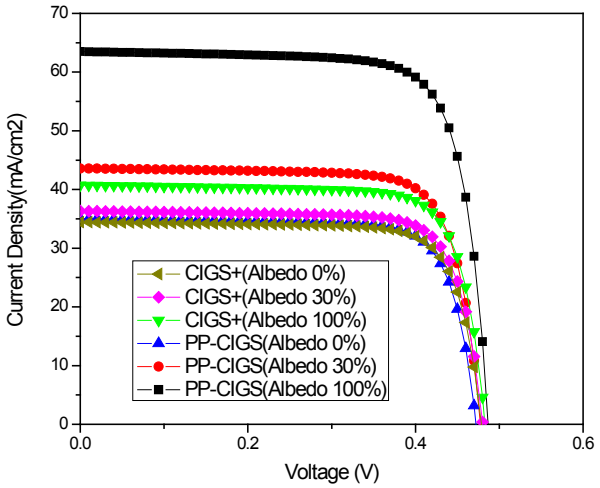

Figure 5. Simulated I-V curves of the CIGS+ and DS-CIGS solar cells, at albedo levels of 0 %, 30 %, and 100 %.

TABLE III.
Efficiencies of the CIGS + and PP-CIGS solar cells.

Solar cell/ albedo	V_{oc} (V)	J_{sc} (mA/cm^2)	FF (%)	η (%)	Energy Boost (%)
CIGS+ / 0%	0.603	29.60	80.80	14.44	NA
CIGS+ / 30%	0.605	31.50	80.70	15.39	6.57
CIGS+ / 100%	0.609	35.95	80.56	17.64	22.16
DS-CIGS/ 0%	0.590	35.10	80.12	16.60	NA
DS-CIGS/ 30%	0.595	42.77	80.47	20.48	23.37
DS-CIGS/ 100%	0.604	60.65	80.99	29.68	78.79

Fig. 5 presents the I-V characteristics of the CIGS+ and DS-CIGS solar cells. Their performances are extracted and listed in Table III. For the CIGS+, the efficiency increases by an additional 3.20 % at an albedo 100 % as compared to its value when the albedo is 0 %. The reason for the smallness of this efficiency increase is that the J_{sc} only increased by 6.35mA/cm^2, indicating a serious current loss for the back illumination. Our DS-CIGS device overcomes this problem, however, as the figure shows. The efficiency of DS-CIGS increased by an additional 13.08 % for an albedo of 100%, as compare to its value at albedo of 0 %. Similarly, J_{sc} also increased substantially, by 25.55mA/cm^2 over the 0 % albedo result. The V_{oc} also increased by 0.14 V. The fill factor (F.F.), increased by 0.87 percentage points. The final result, for a 100 % albedo, is a conversion efficiency (η) of 29.68 % and an energy boost of 78.79 %.

4. Conclusions

We have designed and demonstrated a new Double-sided CIGS solar cell, for improved conversion efficiency in bifacial illumination. Although only snow environments have an albedo approaching 100 %, solar cells can also be used in systems with rear reflectors where the solar cell is elevated. At an albedo of 100 %, the V_{oc}, J_{sc}, FF, η and energy boost reached 0.604 V, 60.65mA/cm^2, 80.99%, 29.68%, and 78.79%, respectively. These results indicate high potential for DS-CIGS cell in bifacial applications.

Acknowledgments

The authors would like to thank the Ministry of Science and Technology, National Center for High-Performance Computing (NCHC) and National Nano Device Laboratories of National Applied Research Laboratories (NARLabs) of Taiwan for providing computational resources and storage resources.

References

[1] Alexander Eeles , Panagiota Arnou, Jake W. Bowers , John M. Walls, Stephen Whitelegg, Paul Kirkham, Cary Allen, Stuart Stubbs, Zugang Liu, Ombretta Masala, Christopher Newman, and Nigel Pickett, "High-Efficiency Nanoparticle Solution-Processed Cu(In,Ga)(S,Se)2 Solar CellsPhotovoltaics", pp. 288-292 (2018).

[2] Rebekah L. Garris, Lorelle M. Mansfield, Brian Egaas, and Kannan Ramanathan, "Low-Cd CIGS Solar Cells Made With a Hybrid CdS/Zn(O,S) Buffer Layer," IEEE Journal of Photovoltaics, pp. 281-285 (2017).

[3] Julie Goffard, Clement Colin, Fabien Mollica, Andrea Cattoni, Christophe Sauvan, and Philippe Lalanne, Jean-Franc¸ois Guillemoles, Negar Naghavi, and Stephane Collin, "Light Trapping in Ultrathin CIGS Solar Cells with Nanostructured Back Mirrors," Photovoltaics, pp.1433-1441 (2017).

[4] K. Aryal, Y. Erkaya, G. Rajan, T. Ashrafee, A. Rockett, Robert W. Collins, and S. Marsillac, "Comparative Study of ZnS Thin Films Deposited by CBD and ALD as a Buffer Layer for CIGS Solar Cell," Photovoltaic Specialists Conference (PVSC), pp. 1101-1104 (2013).

[5] Sharmin Aktar Chowdhury, Md. Shah Alam, "Enhancement of Device Performance with Optimized Absorber Layer in CIGS Solar Cell", Electrical Information and Communication Technologies (EICT), pp. 475-479 (2015).

[6] Samaneh Sharbati and James R. Sites, "Impact of the Band Offset for n-Zn(O,S)/p-Cu(In,Ga)Se2 Solar Cell Photovoltaics", pp. 697-702 (2014).

[7] Marika Edoff, Jonathan Joel, Bart Vermang, Carl Hägglund, "Back Contact Passivation Effects in Bi-Facial Thin CIGS Solar Cells", Photovoltaic Specialist Conference (PVSC), pp. 1-4 (2017).

[8] T. Nakada, Y. Hirahayashi, T. Tokado and D.Ohmori, "Cu(In_{1-x},Ga_x)Se_2 Thin Film Solar Cells Using Transparent Conducting Oxide Back Contacts for Bifacial and Tandem Solar Cells", World Conference on Photovoltaic Energy Conversion, pp. 2880-2884 (2003).

[9] Atlas User's Manual, 4701 Patrick Henry Drive, Bldg. 2 August 26, 2016 Santa Clara, CA 95054.